JUSTC

Article

http://justc.ustc.edu.cn

Received: November 25, 2021; Accepted: January 18, 2022

High-sensitivity double-quantum magnetometry in diamond via quantum control

Yang Dong[1,2] ✉, Haobin Lin[1,2], Wei Zhu[3,4], and Fangwen Sun[1,2]

[1]*CAS Key Laboratory of Quantum Information, University of Science and Technology of China, Hefei 230026, China;*
[2]*CAS Center for Excellence in Quantum Information and Quantum Physics, University of Science and Technology of China, Hefei 230026, China;*
[3]*Hefei National Laboratory for Physical Sciences at the Microscale, University of Science and Technology of China, Hefei 230026, China;*
[4]*Department of Physics, University of Science and Technology of China, Hefei 230026, China*

✉Correspondence: Yang Dong, E-mail: dongy13@ustc.edu.cn

Graphical abstract

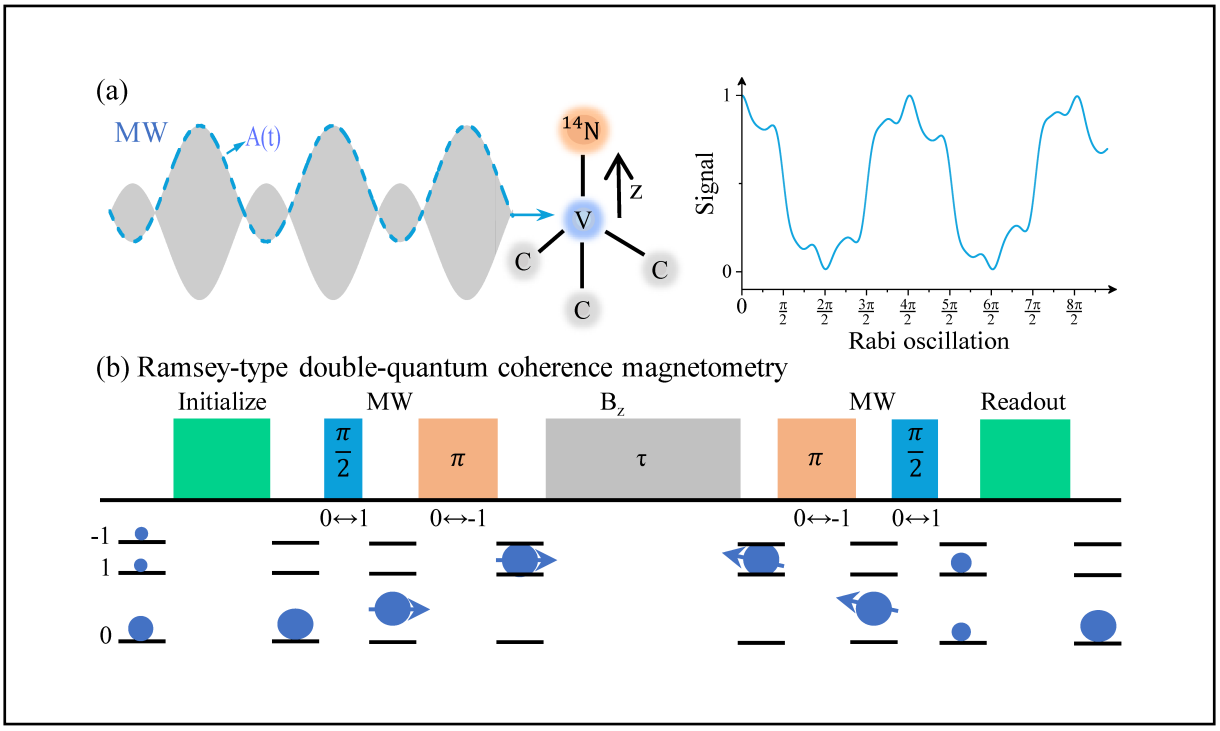

Implement double-quantum magnetometry in diamond with high-fidelity quantum control.

Public summary

- We demonstrate a simple method to synchronously manipulating electron spin of NV center coupling with the nuclear spin in its maximal mixed state by microwave MW amplitude modulation technology.
- The maximum contrast of double-quantum (DQ) magnetometry is realized and the DC magnetic field detection sensitivity is improved over a wide range of bias magnetic field.
- Working in the regime of very low Zeeman splitting, the detection sensitivity is enhanced approximately three times and yield high sensitivity (~200 nT/ Hz) for DC magnetic field detection with DQ pulse sequences, which is prefer to detect nuclear spin signals at zero- and low-field Nano-NMR with NV centers.

Citation: Dong Y, Lin H B, Zhu W, et al. High-sensitivity double-quantum magnetometry in diamond via quantum control. *JUSTC*, **2022**, 52(3): 3. DOI: 10.52396/JUSTC-2021-0249

JUSTC

Article

http://justc.ustc.edu.cn

Received: November 25, 2021; Accepted: January 18, 2022

High-sensitivity double-quantum magnetometry in diamond via quantum control

Yang Dong[1,2] ✉, Haobin Lin[1,2], Wei Zhu[3,4], and Fangwen Sun[1,2]

[1]*CAS Key Laboratory of Quantum Information, University of Science and Technology of China, Hefei 230026, China;*
[2]*CAS Center for Excellence in Quantum Information and Quantum Physics, University of Science and Technology of China, Hefei 230026, China;*
[3]*Hefei National Laboratory for Physical Sciences at the Microscale, University of Science and Technology of China, Hefei 230026, China;*
[4]*Department of Physics, University of Science and Technology of China, Hefei 230026, China*

✉Correspondence: Yang Dong, E-mail: dongy13@ustc.edu.cn

Cite This: *JUSTC*, **2022**, 52(3): 3 (5pp) Read Online

Abstract: High-fidelity quantum operation of qubits plays an important role in magnetometry based on nitrogen-vacancy (NV) centers in diamonds. However, the nontrivial spin-spin coupling of the NV center decreases signal contrast and sensitivity. Here, we overcome this limitation by exploiting the amplitude modulation of microwaves, which allows us to perfectly detect magnetic signals at low fields. Compared with the traditional double-quantum sensing protocol, the full contrast of the detection signal was recovered, and the sensitivity was enhanced three times in the experiment. Our method is applicable to a wide range of sensing tasks, such as temperature, strain, and electric field.

Keywords: double-quantum sensing; nitrogen-vacancy center; quantum control

CLC number: O77+3; TP212 **Document code:** A

1 Introduction

The detection of weak magnetic fields with the nanoscale spatial resolution is a challenging task in biological and physical sciences. In recent years, negatively charged nitrogen-vacancy (NV) centers in diamond have become attractive candidates for solid-state magnetometry[1–5] with high sensitivity and nanoscale resolution, owing to their long coherence time, near-atomic size, as well as optical preparation and readout of NV spin states at room temperature. With suitable double-quantum (DQ) pulse sequences[6–8], the NV center is insensitive to temperature fluctuations but has enhanced target magnetic sensitivity, which takes full advantage of the S=1 spin state nature. Many applications[9,10] utilize NV centers for high-sensitivity DC magnetic-field sensing and wide-field DC magnetic imaging, including the measurements of single-neuron action potentials, current flow in graphene, and paleomagnetism.

For NV magnetometry, conventional NV optical readout exploits the $m_s = \pm 1$ states' higher preference of entering the singlet-state cascade than the $m_s = 0$ state, which leads to a 30% photoluminescence (PL) difference between the "brighter" spin $m_s = 0$ and "darker", $m_s = \pm 1$ state. However, the nonzero host nitrogen nuclear spin of the NV center coupled with its electron spin splits the electron spin level and decreases the signal detection contrast[11] and the sensitivity of the magnetometer[12,13]. In the experiment, such hyperfine effects were eliminated using the dynamic nuclear polarization (DNP) method. The host nitrogen nuclear spin can be optically polarized through excited-level anti-crossing or combined optical, microwave (MW), and radiofrequency (RF) control. However, the bias magnetic field of the DNP method can lead to many undesirable effects during the structural analysis of the molecules[14,15]. This induces a Zeeman interaction, which then dominates the J-coupling, masking crucial information about the chemical bonds. RF control takes a long time[16], which leads to poor detection sensitivity.

In this study, we report a simple method to efficiently solve this problem using MW amplitude modulation technology. For a typical ^{14}NV center in diamond, the ^{14}N spin coupling with electron spin splits it into three energy levels, which leads to a decrease in the readout contrast to one-third. By employing the amplitude modulation of the MW field, we could coherently control the three hyperfine transitions in the experiment. The maximum signal detection contrast was achieved, and the DC magnetic field detection sensitivity was improved. By working in the regime of extremely low Zeeman splitting, the detection sensitivity of a single NV center was enhanced approximately three times, thus yielding a high sensitivity (~200 nT/$\sqrt{\text{Hz}}$) for DC magnetic field detection with DQ pulse sequences. Hence, our method can be easily implemented in every common NV center-based quantum sensing setup and is applicable to low fields.

2 Experiment setup

In the experiment, the NV in the diamond center was addressed using a home-built confocal microscope system. A dry objective lens (N.A. = 0.95 Olympus) focused the 532 nm laser onto a single NV center and collected the emission photon from the NV center. After passing through a long-pass filter (Semrock BLP01-647R-25), the red photons (wavelength ranging from 647 to 800 nm) were collected into a fiber and using by a single-photon counting module (Excelitas Technologies SPCM-AQRH-W5-FC). A copper wire of 20 μm diameter above the bulk diamond was used for the

DOI: 10.52396/JUSTC-2021-0249
JUSTC, **2022**, 52(3): 3

delivery of MW and magnetic fields with a square wave shape to the NV center. The driving MW was generated using an AWG (Keysight M8190a) and amplified using a microwave amplifier (Mini-circuits ZHL-5W-2G-S+). A magnetic field was directly generated using an AWG (Keysight 33522B). The optical, magnetic field and MW pulse sequences were synchronized using a multichannel pulse generator (Spincore, PBESR-PRO-500).

In this experiment, the bulk diamond was produced using chemical vapor deposition growth[17,18], which is grown on type Ib commercial high-pressure high-temperature (HPHT) (100) oriented single crystal diamond of approximate dimensions 3 mm × 3 mm × 0.5 mm from Element 6 corporation. After the growth, the sample was separated from the HPHT diamond substrate by laser cutting, and both sides of the growth plates were polished using a mechanical polisher. Before we used the diamond sample for our experiment, it was cleaned in a mixture of sulfuric and nitric acid (1:2) for 1 h at 200 ℃ and ultrasonically with deionized water, acetone, and isopropanol. The NV center used in this study was formed naturally during the growth of a single-crystal diamond. The abundance of ^{13}C is at the nature level of 1%. The concentration of NV centers is approximately 0.2/μm^3.

In such a system, the Hamiltonian of the ^{14}NV center can be expressed as[18]

$$H_s = DS_z^2 + \gamma_e BS_z + PI_z^2 + \gamma_n BI_z + A_{zz}S_zI_z,$$

where $D = 2.87$ GHz denotes the zero-field splitting of the ground state. S_z and I_z are the electron spins, ^{14}N is the nuclear spin; γ_e, γ_n is the gyromagnetic ratio. A_{zz} is the hyperfine interaction for ^{14}N nuclear spins, and P is the quadrupole splitting of the ^{14}N nuclear spin. We denote the eigenstate of the system Hamiltonian using $|m_s, m_I\rangle$. In the experiment, the observed fluorescence signal, which is related to the population distributions among the $m_s = 0$ and $m_s = \pm 1$ states of the NV center, can be converted to the probability of success of the quantum coherent operation by a linear transformation. Specifically, we first initialized the system into the $m_s = 0$ state by a 532 nm laser pulse and then changed it into the $m_s = \pm 1$ state by MW operation and measured their photon counts (denoted by $n_{\max}$, $n_{\min}$). Hence, the relative population of the $m_s = 0$ state for an unknown state can be expressed as[11] $P_0 = \frac{n - n_{\min}}{n_{\max} - n_{\min}}$, where n is the measured photon count under identical experimental conditions.

3 Experiment results

We applied a small bias magnetic field $B = 21$ Gauss along the NV axis using a permanent magnet, as shown in Fig. 1a. At room temperature, the ^{14}N nuclear spin is in its maximal mixed state; its hyperfine coupling with the electron spin splits the electron energy level into three and decreases the signal contrast. To observe the hyperfine structure, we chose the Rabi frequency ($\Omega_0 = 0.56(2)$ MHz) properly, which corresponds to a time scale for the π pulse of approximately 900 ns, as shown in Fig. 1b. The main noise source is the fluctuations of the photons emitted from the NV centers. From the optically detected magnetic resonance (ODMR) spectrum, we determined the resonant frequencies of the NV center as follows: $f_1 = 2.80920(1)$ GHz ($|0,1\rangle \leftrightarrow |1,1\rangle$), $f_2 = 2.81134(1)$ GHz ($|0,0\rangle \leftrightarrow |1,0\rangle$), and $f_1 = 2.81349(1)$ GHz ($|0,-1\rangle \leftrightarrow |1,-1\rangle$). The contrast of electron-spin nutation is less than 1 because of the unpolarized ^{14}N nuclear spin. If we increase the MW power three times, the contrast of Rabi oscillation is enhanced as shown in Fig. 1c. However, the oscillation frequency component of the signal will increase, which leads to an increase in the complexity of the signal analysis. Moreover, the contrast of Rabi oscillation is still less than 1, which implies that we cannot flip the electron spin perfectly as shown in Fig. 1c. Although increasing the MW power is useful under certain circumstances, it will disturb other states when the intensity becomes comparable to the Zeeman splitting at low-field[19]. A simple single-frequency MW field cannot be used to address three transitions synchronously. The Rabi oscillation becomes complicated under high power driving. The duration time of quantum gate (e.g., $\pi/2$ or π) for sensing protocol, such as Ramsey or spin-echo sensing sequence, is difficult to acquire based on the Rabi oscillation in this case.

We show that the NV center can be perfectly controlled by the amplitude modulation of the MW pulse with an ^{14}N nuclear spin in the maximal mix state. The shaped-driving MW field has a simple analytical expression: $\Omega(t) = A(t)\cos(\omega t)$,

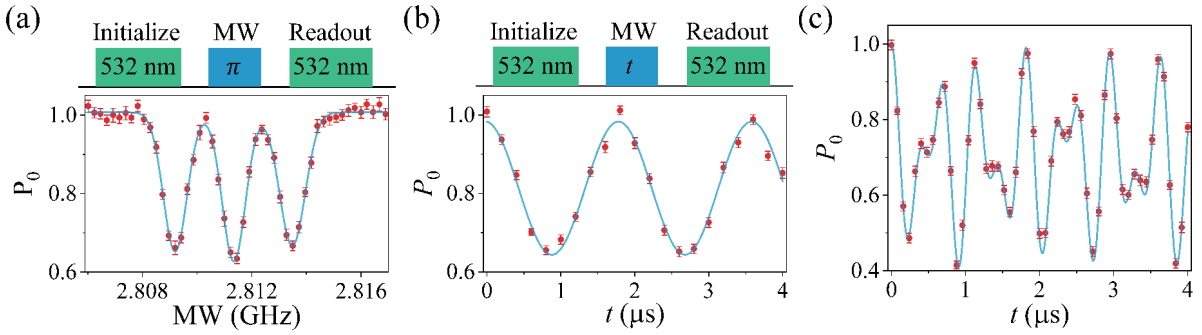

Fig. 1. Coherent operation of a single NV center in diamond. (a) Pulsed ODMR spectrum of a single ^{14}NV center at a bias magnetic field of 21 Gauss. A single resonant spectral line splits into three lines with intervals of 2.16 MHz because of the unpolarized ^{14}N nuclear spin hyperfine coupling with nitrogen NV electron spin. (b-c) Rabi oscillation of electron spin for the transition $|0,0\rangle \leftrightarrow |1,0\rangle$ with different MW power. For low MW power, the Rabi oscillation can be fitted with a simple cosine function. When the MW power is increased three times, the frequency of Rabi oscillation cannot be easily determined for experimental results. The laser power at 532 nm is 0.7 mW in our experiment.

DOI: 10.52396/JUSTC-2021-0249
JUSTC, **2022**, 52(3): 3

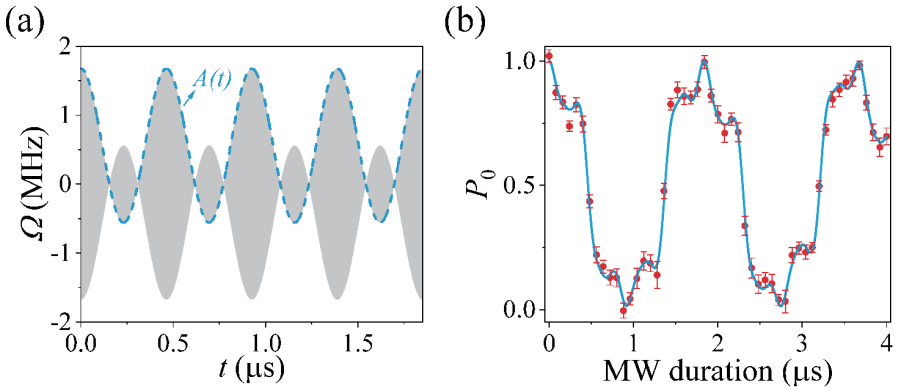

Fig. 2. Rabi oscillation with shaped MW pulse. (a) MW sequence scheme of amplitude modulation. The gray region denotes carrier frequency ($\omega = f_2$). The blue dash line denotes the modulation function $A(t) = \Omega_0[2\cos(\Delta t) + 1]$, where $\Omega_0 = 0.558$ MHz. (b) Rabi oscillation of NV center driving by the amplitude modulation of the MW pulse. The time scale for the π gate is 920 ns.

where $A(t) = \Omega_0[2\cos(\Delta t) + 1]$. Fig. 2a shows the amplitude-modulation MW sequence. In the frequency domain, our MW driving sequence had three components: $\omega, \omega \pm \Delta$. Because only the $\pi/2$ and gates are required for quantum protocols such as Ramsey or spin-echo sequences, we optimized the MW pulse parameters $\Delta = A_{zz} = \sqrt{15}\Omega_0$ to achieve a high control fidelity. When we implement a $\pi/2$ gate with our method, we choose the frequency (ω) of the MW resonance with a target transition of the NV center. The rest of the frequency components detuned with this transition. Hence, the duration of MW can satisfy both conditions: $\Omega_0 t = \pi/2$, $\sqrt{\Omega_0^2 + \Delta^2}t = 2\pi$, which maximally reduces the disturbance of the remaining detuning MW components. We implemented an NV center with a shaped pulse to verify its spin response characteristics and test its control effects. Only one set of MW sources was required in the experiment because only the amplitude of the microwave was modulated in our pulse. Thus, the Rabi oscillation signal has a quasi-periodicity as shown in Fig. 2b. Compared with the traditional rectangular MW pulse method (Figs. 1b and 1c), the contrast of the Rabi oscillation is enhanced.

Because the electron spin of the NV center can be perfectly controlled using our method, sensitivity can also be enhanced. We verified the enhancement of magnetic field detection with a single quantum (SQ) Ramsey sequence, as shown in Fig. 3a. A 532 nm laser was used to initialize the electron spin to $m_s = 0$. Subsequently, a $\pi/2$ gate transfers the quantum sensor into the superposition state $(|0\rangle + |1\rangle)/\sqrt{2}$. The superposition state evolves under magnetic field for time τ and picks up a phase-shift $\phi = \gamma_e B\tau$. Finally, the accumulated phase is coherently converted to a population difference using the $\pi/2$ gate and read out optically. We compared the amplitude modulation control sensing scheme with the conventional single-frequency-controlled scheme using $\Omega_0 =$ 0.558 MHz. As shown in Fig. 3b, Ramsey fringes are detected and fitted with[12] $s = \frac{c}{2}\exp\left[-(t/T_2^*)^2\right]\cos(\gamma_e B\tau) + b$, where c is the contrast and T_2^* is the SQ spin coherence time. The experimental results indicate almost perfect manipulation of the electron spin with our method, and the photon-shot-noise-limited sensitivity of the NV center using the Ramsey sensing

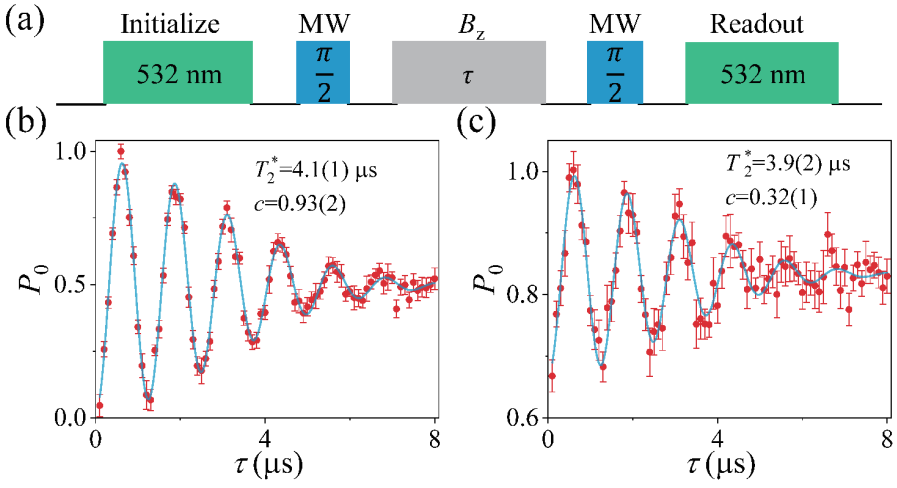

Fig. 3. Ramsey sensing results. (a) Pulse sequence for the Ramsey sensing protocol. A DC magnetic field is applied along the NV center axis. (b–c) Ramsey fringes of the NV center driven with or without amplitude modulation of MW pulse. Here, the MW pulse addresses the target transition $|0,0\rangle \leftrightarrow |1,0\rangle$. The duration time of the $\pi/2$ gate is 460 ns. By fitting experimental results with theory, the coherent time for both cases is $T_2^* \approx 4$ μs. However, the signal contrast of our sharp sequence is improved approximately three times compared with the traditional method. The Rabi frequency for the traditional Ramsey is set as $\Omega_0 = 0.558$ MHz.

DOI: 10.52396/JUSTC-2021-0249
JUSTC, **2022**, 52(3): 3

protocol can be expressed is in direct proportion to the contrast of the detection signal. For a comparison with the original results as shown in Fig. 3c, the main difference is the signal contrast. Thus, the sensitivity enhancement factor can be derived by comparing the differences in contrast.

We further detected DC magnetic field changes by applying DQ Ramsey sensing sequences to the NV center. DQ magnetometry employs the $\{1,-1\}$ subbasis of the NV spin-1 system for quantum sensing. On this basis, noise sources that shift the $|\pm1\rangle$ states in common mode are suppressed by the Zeeman shift between the $|1\rangle$ and $|-1\rangle$ spin states. In addition, the NV DQ spin coherence accumulates phase owing to an external magnetic field at twice the rate of traditional SQ coherence magnetometry[6,7] and provides enhanced susceptibility to target magnetic-field signals as shown in Fig. 4a. DQ Ramsey fringes were detected upon changing the value of the DC magnetic field as shown in Fig. 4b. By applying a DC magnetic field with a fixed value, the accumulated relative phase increases linearly with the sensing time, and the signal difference decreases because the spin coherence is twice as sensitive to magnetic noise, as shown in Fig. 4c. Fig. 4d shows that the relative phase increased linearly with the value of the DC magnetic field when the sensing time was fixed. Similarly, we compared our results with those of the traditional method and observed an improvement in detection signal contrast. The photon shot-noise-limited minimum detectable magnetic field is given by[2,9] $\delta B_{\min} = \sigma_s^N / dS_B$, where σ_s^N is the standard deviation (denoted by the error bar in Fig. 4d) of the DQ Ramsey measurement after N averages and dS_B is the slope of the detection signal variation with B_z. For a short sensing time ($\tau < T^*_{2,DQ}$), $\delta B_{\min}$ decreases with increasing sensing time because of the linear increase in the slope of the detection signal with a given fixed photon fluctuation. For large values of the sensing time, $\delta B_{\min}$ deteriorates rapidly when the NV center coherence time is exceeded. The best DR Ramsey protocol measurement sensitivity with amplitude modulation for all $\pi/2$ and gates was calculated as $\eta = \delta B_{\min}\sqrt{\tau} \sim 200$ nT/$\sqrt{\text{Hz}}$ with $\tau = 1.15$ μs, which is better than the traditional case (~652 nT/$\sqrt{\text{Hz}}$) without amplitude modulation of the MW, as shown in Fig. 4e.

4 Conclusions

In summary, we demonstrated a high-sensitivity DQ Ramsey protocol with full contrast for DC magnetic field sensing using the MW amplitude modulation method. We achieved a sensitivity three times higher than that of the conventional

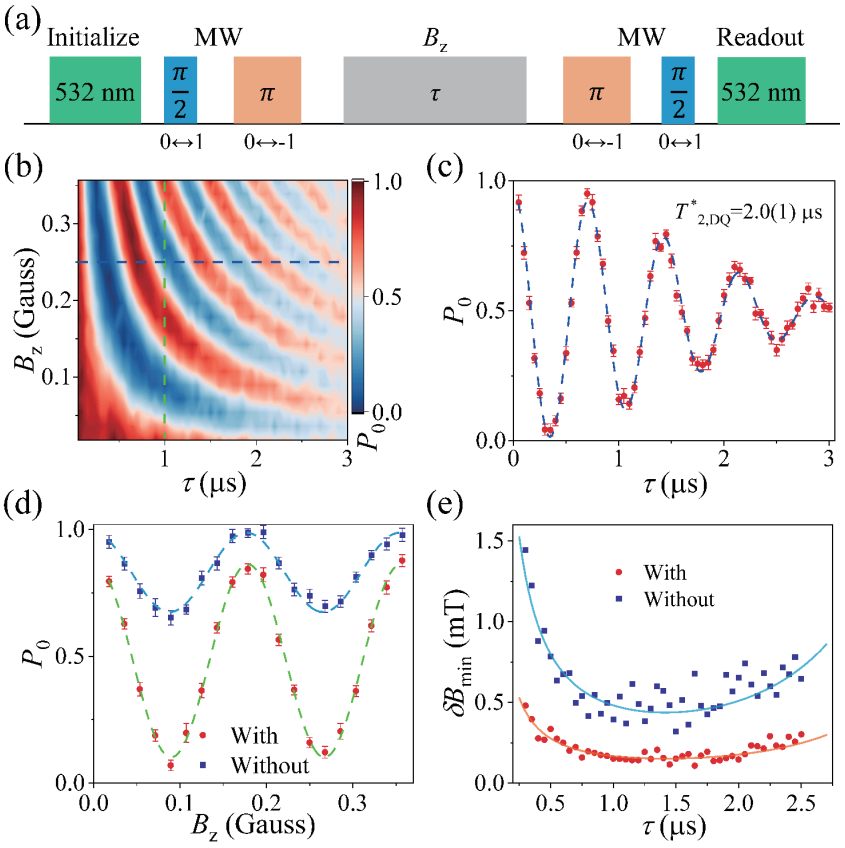

Fig. 4. DQ Ramsey sensing protocol and results. (a) Pulse sequence for the DQ Ramsey sensing protocol. Compared with the SQ Ramsey sequence, the π gate (denoted with orange) needs to be applied after preparing the electron spin into a superposition state $(|0\rangle+|1\rangle)/\sqrt{2}$. The frequency of the π gate is in resonance with the transition $|0,0\rangle \leftrightarrow |-1,0\rangle$. Then, the probe state $(|-1\rangle+|1\rangle)/\sqrt{2}$ for the detection of the DC magnetic field is obtained. (b) DQ Ramsey sensing results as a function of sensing time (τ) and DC magnetic-field change. (c) DQ Ramsey results with fixed amplitude of DC magnetic field, which corresponds to the blue dashed line in Fig. 4 (b). The coherence time for DQ Ramsey is $T^*_{2,DQ} \approx 2$ μs. (d) DQ Ramsey results (denoted by red dots) as a function of the amplitude of DC magnetic field with fixed sensing time (τ=1 μs) for out shaped MW pulse. The blue square corresponds to the rectangular MW pulse. (e) Measured sensitivity of a single NV spin magnetometer over a range of sensing time after repeating $N = 1.5\times10^6$ times.

DOI: 10.52396/JUSTC-2021-0249
JUSTC, **2022**, 52(3): 3

scheme. This method works similarly to other spin-spin coupling-inducing splitting systems. Moreover, our scheme can also be used for high-sensitivity AC magnetic field detection with prolonged decoherence times by dynamical decoupling[20,21] at a low-bias magnetic field. Hence, our study brings us a step closer to the ultimate goal of investigating *J*-coupling in molecules or various condensed matter experiments via the NV center, as it is now possible to do so even in the absence of a bias magnetic field.

Acknowledgements

This work was supported by the Fundamental Research Funds for the Central Universities (WK2030000020) and the National Natural Science Foundation of China (12005218).

Biographies

Yang Dong received his PhD degree in Physics from University of Science and Technology of China (USTC). He is currently a Research Associate at Department of Optical Engineering, USTC. His major research interests focus on the quantum sensing and quantum coherent operation with a solid spin in diamond.

References

[1] Degen C L, Reinhard F, Cappellaro P. Quantum sensing. *Rev. Mod. Phys.,* **2017**, *89*: 035002.
[2] Barry J F, Schloss J M, Bauch E, et al. Sensitivity optimization for NV-diamond magnetometry. *Rev. Mod. Phys.,* **2020**, *92*: 015004.
[3] Chen X, Zou C, Gong Z, et al. Subdiffraction optical manipulation of the charge state of nitrogen vacancy center in diamond. *Light Sci. Appl.,* **2015**, *4*: e230.
[4] Chen X D, Wang E H, Shan L K, et al. Focusing the electromagnetic field to $10^{-6}\lambda$ for ultra-high enhancement of field-matter interaction. *Nat. Commun.,* **2021**, *12*: 6389.
[5] Dong Y, Du B, Zhang S C, et al. Solid quantum sensor based on nitrogen-vacancy center in diamond. *Acta. Phys. Sin.,* **2018**, *67*: 160301.
[6] Fang K, Acosta V M, Santori C, et al. High-sensitivity magnetometry based on quantum beats in diamond nitrogen-vacancy centers. *Phys. Rev. Lett.,* **2013**, *110*: 130802.
[7] Mamin H J, Sherwood M H, Kim M, et al. Multipulse double-quantum magnetometry with near-surface nitrogen-vacancy centers. *Phys. Rev. Lett.,* **2014**, *113*: 030803.
[8] Bauch E, Hart C A, Schloss J M, et al. Ultralong dephasing times in solid-state spin ensembles via quantum control. *Phys. Rev. X,* **2018**, *8*: 031025.
[9] Maze J R, Stanwix P L, Hodges J S, et al. Nanoscale magnetic sensing with an individual electronic spin in diamond. *Nature,* **2008**, *455*: 644–647.
[10] Balasubramanian G, Chan I Y, Kolesov R, et al. Nanoscale imaging magnetometry with diamond spins under ambient conditions. *Nature,* **2008**, *455*: 648–651.
[11] Dong Y, Zheng Y, Li S, et al. Non-Markovianity-assisted high-fidelity Deutsch–Jozsa algorithm in diamond. *npj Quantum Inf.,* **2018**, *4*: 3.
[12] Dong Y, Zhang S C, Lin H B, et al. Quantifying the performance of multi-pulse quantum sensing. *Phys. Rev. B,* **2021**, *103*: 104104.
[13] Li C H, Dong Y, Xu J Y, et al. Enhancing the sensitivity of a single electron spin sensor by multi-frequency control. *Appl. Phys. Lett.,* **2018**, *113*: 072401.
[14] Kong F, Zhao P J, Ye X Y, et al. Nanoscale zero-field electron spin resonance spectroscopy. *Nat. Commun.,* **2018**, *9*: 1563.
[15] Jiang M, Frutos R P, Wu T, et al. Magnetic gradiometer for the detection of zero- to ultralow-field nuclear magnetic resonance. *Phys. Rev. Appl.,* **2019**, *11*: 024005.
[16] Xu N Y, Tian Y, Chen B, et al. Dynamically polarizing spin register of N-V centers in diamond using chopped laser pulses. *Phys. Rev. Appl.,* **2019**, *12*: 024055.
[17] Zhao B W, Dong Y, Zhang S C, et al. Improving the NV generation efficiency by electron irradiation. *Chin. Opt. Lett.,* **2020**, *18*: 080201.
[18] Dong Y, Zhang S C, Zheng Y, et al. Experimental implementation of universal holonomic quantum computation on solid-state spins with optimal control. *Phys. Rev. Appl.,* **2021**, *16*: 024060.
[19] Cerrillo J, Casado S O, Prior J. Low field nano-NMR via three-level system control. *Phys. Rev. Lett.,* **2021**, *126*: 220402.
[20] Dong Y, Chen X D, Guo G C, et al. Reviving the precision of multiple entangled probes in an open system by simple π-pulse sequences. *Phys. Rev. A,* **2016**, *94*: 052322.
[21] Dong Y, Xu J Y, Zhang S C, et al. Composite-pulse enhanced room-temperature diamond magnetometry. *Funct. Diamond,* **2021**, *1*: 125–134.

DOI: 10.52396/JUSTC-2021-0249
JUSTC, **2022**, 52(3): 3